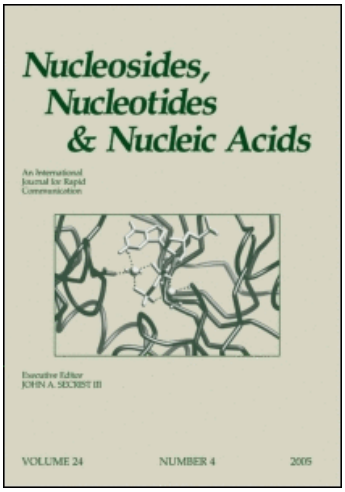

Nucleosides, Nucleotides and Nucleic Acids
Publication details, including instructions for authors and subscription information:
http://www.informaworld.com/smpp/title~content=t713597286

Side-Chain Conformational Restriction in Template-Competitive Inhibitors of *E. coli*DNA Polymerase I Klenow Fragment: Synthesis, Structural Characterization and Inhibition Activity

Michael B. Doughty[a]; Karam Aboudehen[a]; Garland Anderson[a]; Ke Li[a]; Bob Moore II[ab]; Tina Poolson[a]
[a] Department of Chemistry and Physics, Southeastern Louisiana University, Hammond, Louisiana, USA [b] Department of Pharmaceutical Sciences, University of Tennessee Health Science Center, Memphis, Tennessee, USA

Online publication date: 11 November 2004

To cite this Article Doughty, Michael B. , Aboudehen, Karam , Anderson, Garland , Li, Ke , Moore II, Bob and Poolson, Tina(2004) 'Side-Chain Conformational Restriction in Template-Competitive Inhibitors of *E. coli*DNA Polymerase I Klenow Fragment: Synthesis, Structural Characterization and Inhibition Activity ', Nucleosides, Nucleotides and Nucleic Acids, 23: 11, 1751 — 1765
To link to this Article: DOI: 10.1081/NCN-200034042
URL: http://dx.doi.org/10.1081/NCN-200034042

NUCLEOSIDES, NUCLEOTIDES & NUCLEIC ACIDS
Vol. 23, No. 11, pp. 1751–1765, 2004

Side-Chain Conformational Restriction in Template-Competitive Inhibitors of *E. coli* DNA Polymerase I Klenow Fragment: Synthesis, Structural Characterization and Inhibition Activity[#]

Michael B. Doughty,[1,*] Karam Aboudehen,[1] Garland Anderson,[1] Ke Li,[1] Bob Moore II,[1,2] and Tina Poolson[1]

[1]Department of Chemistry and Physics, Southeastern Louisiana University, Hammond, Louisiana, USA
[2]Department of Pharmaceutical Sciences, University of Tennessee Health Science Center, Memphis, Tennessee, USA

ABSTRACT

Nucleotide triphosphate α-(4-azidophenyl)-1,N^6-etheno-dATP **3** and its monophosphate **3m** were synthesized by condensation of 2-halo-2-(4-azidophenyl)acetaldehyes with dATP and dAMP, respectively. Structure analysis shows that the azidophenyl side chain is attached to the α-position of the etheno ring (i.e., the carbon attached to N1 of the purine), and conformation calculations show minima in the etheno-phenyl bond rotation at 50 and 130° where the bulk of the phenyl ring projects out from the plane of the etheno group. Like DNA Pol inhibitor 2-(4-azidophenacyl)thio-2′-deoxyadenosine 5′-triphosphate **1**, nucleotide **3** is a template-competitive DNA polymerase inhibitor (TCPI), with a competitive Ki for Pol I KF of 3.41 μM, but has only weak activity as an HIV RT inhibitor relative to the template-competitive reverse

[#]This work was funded in part by the Louisiana Board of Regents 044UG-02 and the National Institutes of Health GM067686.
[*]Correspondence: Michael B. Doughty, Department of Chemistry and Physics, Southeastern Louisiana University, SLU Box 10878, Hammond, LA 70402, USA; Fax: (985) 549-5126; E-mail: mdoughty@selu.edu.

DOI: 10.1081/NCN-200034042
1525-7770 (Print); 1532-2335 (Online)

transcriptase inhibitor 2-(4-azidophenacyl)thio-1,N^6-etheno-2′-deoxyadenosine 5′-triphosphate **2**. Additionally, **3** photoinactivates KF in a time-dependent manner, confirming the kinetic data that **3** binds to the free form of KF. The TCPI activity of **3** provides evidence for an extended side chain conformational preference in the combined substrate polymerase inhibitors.

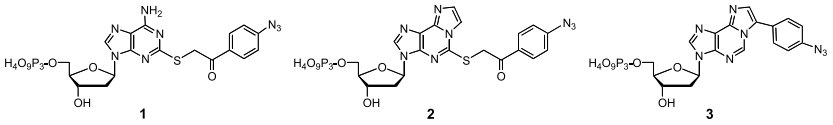

1 **2** **3**

Key Words: DNA polymerase inhibitors; Reverse transcriptase inhibitors; Klenow fragment.

INTRODUCTION

We previously reported inhibitors of DNA polymerase I Klenow fragment (KF) and HIV-1 reverse transcriptase (RT) based on 2-substituted dATP derivatives. These nucleotide inhibitors bind to the free enzyme in competition with template-primer. These so-called template-competitive inhibitors of Pol I and reverse transcriptase differ primarily based on the absence or presence of a 1,N^6-etheno group. Thus the dATP analog **1** is a KF inhibitor with a competitive Ki versus template/primer of 2.1 μM,[1] and its exact etheno analog **2** is a template-competitive reverse transcriptase inhibitor (TCRTI) versus HIV RT, with a competitive Ki versus template-primer of 10 μM.[2]

The initial template-competitive polymerase inhibitor (TCPI) **1** was designed as a photoprobe based on a thermodynamic model for substrate binding to DNA polymerase developed by Doronin and Kolocheva.[3,4] In our model, the dATP moiety of **1** binds to the dNTP site and the 2-phenacylthio side chain binds to a lipophilic pocket in the template binding site predicted by the thermodynamic model and observed by photolabeling (Fig. 1A).[5] The phenacyl side chain of **1** increases binding to the free form of KF by about 20 fold relative to shorter side chain or natural dNTPs.[1] However, this model was unable to account for the activity of the etheno derivative **2** in the TCRTI series, where the combination of the 2-etheno and 2-phenacylthio side chain increased potency as TCRTIs by >300-fold over natural dNTPs and **1** but reduced polymerase inhibition activity.[2,6] Conformational analysis led us to propose that the main effect of the etheno group in **2** is to shift the 2-side chain conformational equilibrium to a 180° Ψ_1 (N1-C2-S-CH_2) torsional angle (Fig. 1B), whereas Ψ_1 in TCPI **1** is 90°, allowing the side chain to project out from the adenine base.[7]

As a test of this conformational hypothesis, we designed TCPI **3**, where the side chain is a phenyl ring appended to the α position of the etheno group, and additionally contains an azido group as a photoprobe for independent analysis of binding interactions. This conformationally restricted analog has the 1,N^6-etheno group of TCRTI **2** but the side chain, appended to the etheno group, cannot adopt the same conformation proposed for the side chain of **2**; in fact, the phenyl ring in **3** is rigidly held even relative to the 2-side chain in **1**. One negative aspect of this design is the decreased length of the side chain in **3**, about 2 Å, relative to the proposed side chain

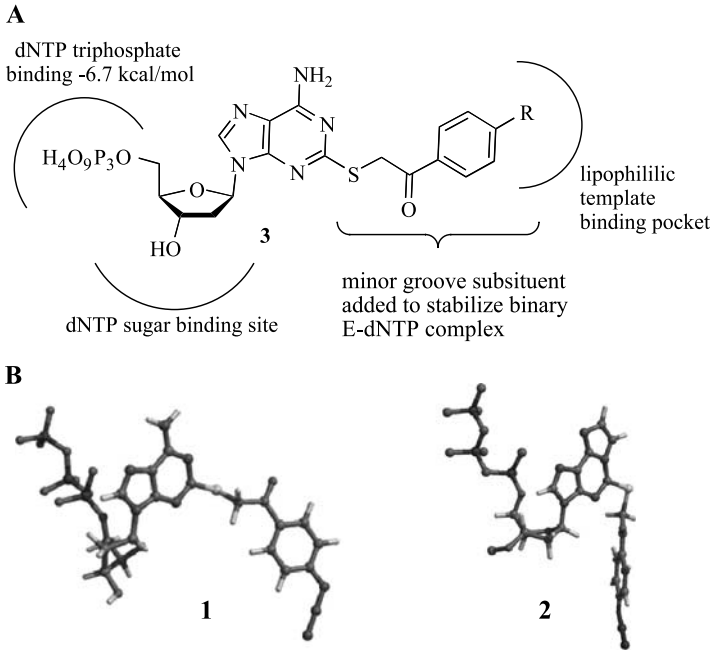

Figure 1. **A** (Top): Binding model proposed for the interaction of template-competitive DNA polymerase inhibitor **1** with the Klenow Fragment; **B** (Bottom): Proposed active structures of TCPI **1** (top) and TCRTI **2** (bottom).

extension in **1**. In the present communication we report the synthesis, structure, and enzyme inhibitory activities of the side-chain restricted TCPI **3**.

RESULTS AND DISCUSSION

TCPI 3 Synthesis and Photochemistry

In general, α-substituted-1,N^6-etheno-2′-deoxyadenosine 5′-triphosphate analogues are prepared by condensation of α-halogenated phenylacetaldehydes with dAMP or dATP as the key reaction. The synthesis of α-halogenated substituted phenylacetaldehydes is depicted in Scheme 1. The 4-azidophenethyl alcohol (**5**), prepared from 4-amino-phenethyl alcohol by the general method of Lewis et. al.,[8] was

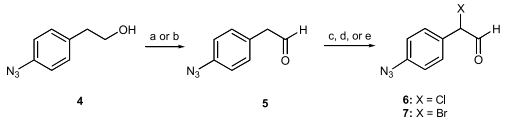

a) i) oxalyl chloride, DMSO, -78 °C; ii) Et_3N; b) PDC, CH_2Cl_2; c) *t*-butylhypochlorite, HOAc; d) NBS, *p*-toluene sulfonic acid (cat.), THF; e) Br_2, CCl_4.

Scheme 1. Synthesis of side chain precursors.

converted to the phenylacetaldehyde derivative by two methods, the Swern oxidation with DMSO and oxalyl chloride[9] and oxidation using pyridinium dichromate (PDC),[10] followed by silica gel chromatography purification. In the presence of the *para*-azido group, the oxidation reaction needs to be conducted in very mild conditions to avoid decomposition of the product. Both PDC and Swern oxidation selectively oxidized **4** to 4-azidophenylacetaldehyde (**5**) without affecting the azido group. However, higher yields were obtained with PDC because the base used in the Swern oxidation, e.g., triethylamine, caused decomposition of the product, while PDC oxidation requires neither strongly basic nor acidic conditions.

Phenylacetaldehydes are halogenated using N-bromo succinimide (NBS), bromine or *t*-butyl hypochlorite (Scheme 1). Hanze et al. reported a one step oxidation/α-halogenation of 3-hydroxysteroids using *t*-butyl hypochlorite.[11] However, when phenethyl alcohol was treated with *t*-butyl hypochloric acid, no reaction was observed, although reaction of benzyl alcohol with *t*-butyl-hypochlorite generated the corresponding aldehyde, and chlorination of phenylacetaldehyde by *t*-butyl hypochlorite in acetic acid generated α-chloro-phenylacetaldehyde. Alternatively, bromination of phenylacetaldehyde with bromine or NBS both generated α-bromo-phenylacetaldehyde in satisfactory yield.

The preparation of 2-halo-2-(4-azidophenyl)acetaldehydes was problematic owing to the extremely poor stability of the product. Chlorination of 4-azido-phenyl-acetaldehyde (**5**) by t-butyl hypochlorite suffered from low yield and poor reproducibility due to significant decomposition under the reaction conditions. Formation of the corresponding carboxylic acid (about 30% based on ^{1}H-NMR) was observed in the chlorination of **6**, although the byproduct did not interfere with the coupling reaction with dATP or dAMP. Additionally, bromination of **5** was accomplished by reaction with NBS in THF only in the presence of a catalytic amount of *p*-toluenesulfonic acid. The bromination usually took 0.5 to 1 hr at room temperature in the presence of *p*-toluenesulfonic acid, while no reaction occurred in the absence of the catalyst. Compounds **6** and **7** were extremely unstable, and extraction with sodium bicarbonate solution or purification on a silica column caused decomposition. Therefore, both **6** and **7** were prepared fresh and carried to the next step without purification.

Treatment of dAMP and dATP with an excess of **6** or **7** in aqueous acetonitrile (50%) generated nucleotides **3m** and **3**, respectively, in about 20% yield (Scheme 2).

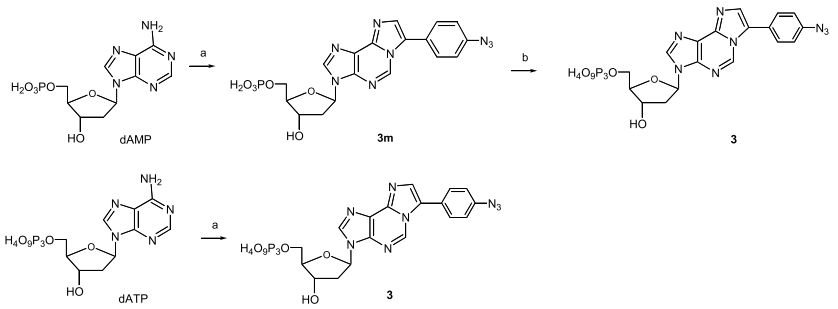

a) **6** or **7** in 50% aqueous CH_3CN, 37°C, 16 hr; b) i) $(PhO)_2P(O)Cl$, $(C_4H_9)_3N$, dioxane; ii) $H_4P_2O_7$-$[(C_4H_9)_3N]_{1.5}$, $(C_4H_9)_3N$, pyridine.

Scheme 2. Synthesis of α-substituted ethenoadensoine analogs.

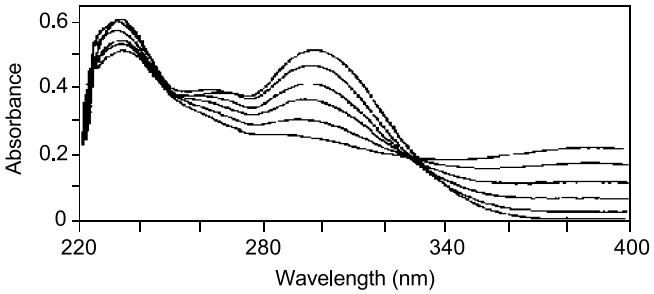

Figure 2. Photodecomposition of **3** at 3000 Å. Aliquots of the photolysis reaction were taken at times (from top to bottom at 298 nm) 0, 0.25, 0.5, 1.0, 2.0, and 4.0 min, and spectra of the aliquots were taken in 0.1 M HCl.

The low yield of this reaction was probably related to the extremely poor stability of 2-halo-2-(4-azidophenyl)acetaldehyde. The yield was very low (<10%) when the reaction was carried out in H_2O, and no product was formed in aqueous 50% DMF. Alternatively, **3** can be prepared from **3m** by activation with phenyl phosphoryl chloride and cleavage with pyrophosphate.[2]

The photo-activity of **3** was examined by monitoring UV absorbance changes upon irradiation at 3000 Å. As shown in Fig. 2, compound **3m** has an absorption maxima at 298 nm, corresponding to the maximum absorption of the electron-deficient phenacylazides in both **1** and **2**.[1,6] Overlay of the UV spectra taken at different times of irradiation showed isobestic points at 250 and 330 nm, indicating a single reaction pathway for the photodecomposition of the aryl azide group. Photodecomposition followed first-order kinetics, with a half-life of 0.9 min, which correlates well with the $t^1/_2$ of 0.6 min for the electron-deficient phenacylazide in **2**.[6] Our results show that the photodecomposition is significantly faster in quartz cuvettes than in pyrex and clear plastic tubes (data not shown). Therefore, all photolysis experiments were conducted in water-jacketed quartz cuvettes silanized in order to prevent nonspecific absorption of protein to the glass surface.

Structure and Conformational Properties of TCPI 3

The reaction of adenine nucleotides with α-halo-acetaldehyde is suggested to occur by initial alkylation at N-1 of the adenosine ring followed by ring closure and dehydration based on alkylation studies in the 2-aminopyridine series.[12] The regiochemistry of the substitution groups in the products were assigned based on this mechanism. For example, when cAMP is reacted with α-bromoacetophenone, the structure of the product (13% yield) is assigned to have the phenyl group at the α position,[13,14] while when reacted with α-bromo-phenylacetaldehyde, the product is assigned as α phenyl-etheno-cAMP.[14]

The regiochemistry of the phenyl group in the $1,N^6$-etheno-dATP derivatives was examined by difference NOE spectra of α-phenyl-$1,N^6$-etheno-dAMP synthesized from condensation of dAMP with α-bromo-2-phenylacetaldehyde (data not shown). Observed NOE enhancement of the *ortho* phenyl protons on selective irradiation of the

C2 proton of the purine ring proves that phenyl ring is on the α-carbon (connected to N1), placing the *ortho* protons within at least 5 Å of C2. Thus the phenyl ring side chain of **3** projects into the minor groove region of the purine ring as suggested by the structures shown.

The orientation of the phenyl ring relative to the $1,N^6$-etheno-adenine ring was examined by calculation of the potential energy using a grid search method pushing the psi angle only from 0 to 180° in 5° increments (a 360° rotation is not required because of the planar symmetry of the two ring systems). As shown in Fig. 3A, two energy minima at 50 and 130° were observed, and two energy maxima were observed, one at 0/180° where the planes of the two rings are parallel, and a second at 90° where the planes of the two rings are perpendicular, with the parallel orientation being the highest energy conformation. This conformational preference is a combined effect of the destabilizing steric interaction between the ortho-phenyl and ring protons and stabilizing π-electron overlap between the phenyl and etheno-adenosine rings, both in

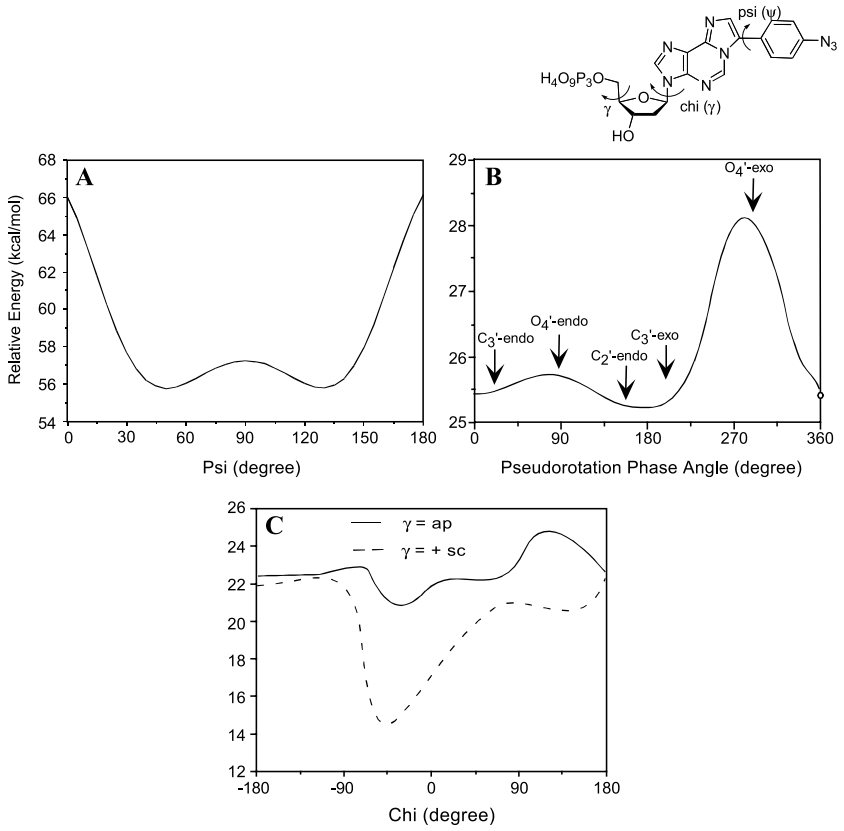

Figure 3. Conformational analysis of the structure of **3**. **A**: Rotation of Psi (the α-etheno-phenyl bond) from 0 to 180°; **B**: Pseudorotation cycle for sugar conformation; **C**: Rotation of the glycosidic bond Chi ($C_{1'}$–N9) from −180 to 180° at two conformations of gamma ($C_{4'}$–$C_{5'}$).

the parallel orientation. Because the phenyl ring adopts a pseudo antiparallel orientation, the bulk of the phenyl ring extends out from the plane of the etheno ring. In addition, rotation of this single bond does not change the relative position of the *para*-substituted azido group relative to the base.

The conformational state of the furanose ring of nucleotide **3** was examined by computation of relative energy as a function of pseudorotation phase angle P.[15] Grid searches were performed in which each endocyclic torsional angle of the furanose ring was driven from $-40°$ to $40°$ by an increment of $3°$ with torsional angles χ and γ starting at *anti* and +sc, respectively. Pseudorotational phase angle P values for each conformation were then calculated to give the energy profile for the entire pseudorotational pathway shown in Fig. 3B. As with TCRTI **2** reported earlier,[7] two energy minima at C_3'-endo ($P \approx 10$) and C_3'-exo/C_2'-endo twist ($P \approx 180$) were observed for **3,** and the minimum at the twist conformation was broad and included $C_{2'}$-endo and $C_{3'}$-exo. A western potential energy barrier (P = 270) of about 3 kcal/mole and an eastern energy barrier (P = 90) of about 0.5 kcal/mol was also observed. These results are consistent with reported furanose conformational preferences, particularly with that found for TCPI **1**,[5] indicating that the structural modifications on the adenine ring in **3** do not exert a major effect on the conformational states of the furanose ring.

Nucleotide geometry is affected by glycosidic torsional angle chi (χ), which changes the orientation of the base relative to the sugar and phosphate moieties. Therefore, energy profiles for **3** relative to χ were examined using grid searches in which χ was driven from $-180°$ to $180°$ by an increment of $5°$. The conformation of the furanose ring was first set at $C_{3'}$-endo and the torsional angle γ at either +sc or ap but not $-$sc since the later is rarely observed.[15] Shown in Fig. 3C are the energy profiles of **3** as a function of χ with γ at ap or +sc. The +sc conformation is favored over the ap conformation and the energy-minimum fell in the range corresponding to the high *anti* conformation. This minimum energy conformation is also consistent with the preferred conformations for the DNA polymerase inhibitor **1**[5] and the reverse transcriptase inhibitor **2**.[7]

Reversible and Irreversible Enzyme Inhibition

The Lineaweaver-Burk plot illustrated in Fig. 4 demonstrates that **3** is a competitive inhibitor of the Klenow Fragment versus template/primer, and the average Ki of 3.41 μM is about 10 times the activity of natural dNTPs such dATP as measured using steady state kinetics with non-complementary template/primer. A summary of the kinetic data is given in Table 1. Nucleotide **3** is nearly equipotent with **1** as a KF inhibitor, and the steady state kinetics for **3** are much cleaner. Although **1** showed mixed competitive inhibition versus template/primer,[1] the inhibition data with **3** for all three experiments fit best to the competitive model even when challenged in a mixed inhibition model. These results indicate that TCPI **3** binds to the free enzyme form of KF in competition with template/primer, and does not bind to the binary enzyme-template/primer complex as a dNTP substrate.

The inhibitory activities of **3** and dATP as a control versus HIV-1 RT are compiled in Table 1; the data are presented as IC_{50}'s because of the weak activity. Control dATP had no inhibitory effect up to 300 μM, indicating an $IC_{50} > 3$ mM, whereas **3** had weak activity with $IC_{50} = 121$ μM. The phenyletheno **3** follows the activity profile observed for the polymerase inhibitors upon which it was designed, with a Pol selectivity ratio of

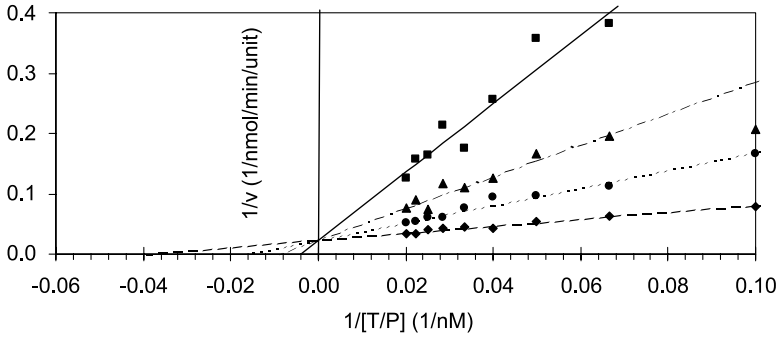

Figure 4. Kinetic pattern for inhibition of Klenow fragment by **3** versus variable template/primer poly(dA) · (dT_{10}) at inhibitor concentrations of 19 (circle with solid line), 13 (triangles with dot-dash line), 6 (circles with dotted line), and 0 (diamonds with dash line) μM.

33 (Table 1). This TCPI selectivity indicates that the side chain conformation, with an extended conformation being preferred in the polymerase inhibitors, and not the absence or presence of the etheno ring, is determinant of enzyme selectivity and activity in this series.

In design, an anchoring interaction of both the TCPIs and the TCRTIs is binding of the triphosphate to the triphosphate coordination site in the dNTP binding site. Thus photoinactivation of and photoincorporation of **1** into KF requires magnesium ion and is inhibited by dATP as well as template/primer.[1,5] The monophosphate analogs of **1** and **2** as well as their derivatives are inactive as inhibitors, certainly since they lack the ability to complex magnesium either in solution or at the triphosphate binding site,[2,5] and in crystal structures of ternary complexes of both DNA polymerase β and HIV-1 reverse transcriptase, the triphosphates are complexed to two magnesium ions.[16,17] Likewise, **3m**, the monophosphate of TCPI **3**, is inactive at its solubility limit as an

Table 1. Summary of inhibition data.

	Inhibition constant (μM)		
Inhibitor	HIV-1 RT	DNA Pol I Klenow	Pol I inhibition selectivity
1	>3000[a]	2.11[b]	1430
2	10[c]	92[c]	0.109
3	121 ± 10.6[d]	3.41 ± 0.12[e]	35
3m	NA[f]	NA[f]	NA[e]
dATP	>3000[f]	34.8 ± 2.52[e]	86

[a]No activity observed in IC_{50} assays up to 300 μM (3 mM magnesium), so activity must be greater than 10 times that maximum.
[b]Competitive Ki's taken from Ref. [1].
[c]Competitive Ki's taken from Ref. [2].
[d]IC_{50} data (average of triplicate determinations).
[e]Competitive Ki's from steady-state kinetic studies (average of triplicate determinations).
[f]No activity at highest concentration available for testing.

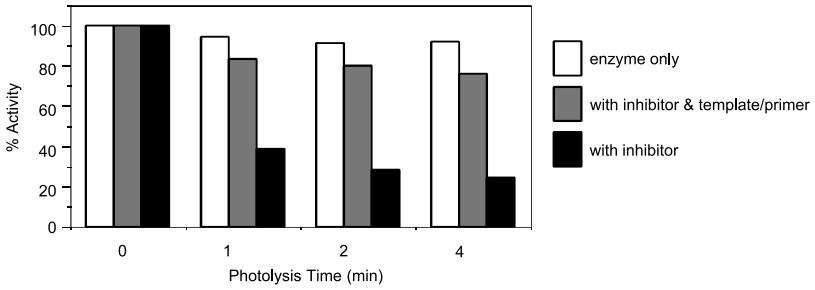

Figure 5. Photoinactivation of KF by TCPI **3** and protection by substrate. In each experiment, Klenow fragment, with and without 100 μM inhibitor **3**, and in the presence of saturating poly(dA)–$(dT)_{10}$, were photolyzed at 3000 Å for the indicated times. Activity assays were performed as describe in experimental.

inhibitor of both KF and RT (Table 1). Thus by this criterion **3** also anchors at the triphosphate site as originally proposed in the binding model for **1** (Fig. 1A).

Irradiation of KF at 3000 Å in the presence of **3** results in a time-dependent loss of polymerase activity with only 24% activity remaining at 4 min (Fig. 5). Saturating template/primer poly(dA) · $(dT)_{10}$ protected 75% of KF from photoinactivation by **3**. This behavior is very similar to the activity of inhibitor **1** versus KF[5] and of **2** versus RT.[6] This photoinactivation data is further supporting evidence that TCPI **3** specifically binds to the free form of KF at a binding site that simultaneously includes part(s) of the dNTP and template/primer binding sites.

CONCLUSIONS

The original TCPI **1** was designed as a KF affinity probe that would bind with good affinity to the dNTP site. Because dNTPs as DNA polymerase affinity probes suffer from weak affinity and poor covalent labeling, the 2-phenacylthio side chain was appended to the minor groove edge of the purine to stabilize binding by interaction at the template site. The 20-fold increase in binding activity to the free enzyme, 100% photolabeling with protection by both template/primer and dATP, and finally affinity labeling in the template site, provided strong evidence for the model.[1,5] But the 40-fold poorer activity of the etheno analog **2** as a TCPI forced us to reexamine the model.

TCPI **3** is truly a template-competitive inhibitor of KF in that it both competes with template/primer in kinetic inhibition assays and efficiently photoinactivates the free form of KF. The conformational properties of **3** include classic nucleotide parameters with C3′-endo sugar conformation, a high-anti glycosidic bond, and a preferred +sc phosphate conformation. Most importantly, the psi bond rotation minima at 50 and 130° indicate that the bulk of the phenyl ring projects out from the plane of the etheno ring. The activity of **3** is 10-fold greater than dNTPs as a TCPI in binding to the free enzyme form of KF, indicating that the etheno itself is not detrimental to KF inhibitory activity; indeed, the near equipotent activity of the restricted analog **3** and the phenacyl analog **1** suggests a side chain conformation that is fully extended in the TCPI series. The slightly weaker activity of **3** vs **1** as a TCPI is likely due to the

decreased length of the phenyl ring side chain in **3**, and we are currently synthesizing analogs of **3** with increasing size at the 4 position of the phenyl ring to increase the TCPI activity in this side chain restricted polymerase inhibitor series.

EXPERIMENTAL METHODS

Materials and Methods

Chemicals and solvents of reagent grade were purchased from commercial suppliers and were used without purification except as follows: NBS was crystallized from water; tetrahydrofuran (THF) was distilled from sodium/benzophenone prior to use; and t-butyl hypochlorite was prepared by the method of Teeter.[18] HIV-1 RT was purchased from Worthington (Lakewood, NJ), and the Klenow fragment of DNA polymerase I was purchased from United States Biochemical Corporation (Cleveland, Ohio). Polynucleotides, oligonucleotides and nonradioactive nucleotides were purchased from Pharmacia (Piscataway, NJ). Tritiated thymidine ([^{3}H]TTP) was purchased from DuPont New England Nuclear (Boston, MA). Bovine serum albumin (BSA) was purchased from Sigma (St. Louis, MO).

Enzyme concentration was measured using Pierce BCA protein assay reagent (Pierce Chemical Co., Rockford, IL) relative to BSA as standard. Measurement of UV absorbance on micro-titer plates was performed in a Bio-Tek Powerwave XS Microplate Reader (Menlo Park, CA). Proton (^{1}H) nuclear magnetic resonance spectra were recorded on General Electric QE-300 and Varian VXR-500S 500 MHz instruments at the University of Kansas NMR Laboratory. Chemical shifts are reported as parts per million (ppm) relative to the $CHCl_3$ peak (= 7.24) in $CDCl_3$ and HOD peak (δ = 4.80) in D_2O. Mass spectra (MS) data for electron ionization and chemical ionization were obtained on a Nermag R10-10 quadruple GC/MS system at the University of Kansas Mass Spec Laboratory. Positive and negative fast atom bombardment (FAB) MS were obtained on a VG Analytical ZAB spectrophotometer. Infrared spectra (IR) were determined on a Perkin–Elmer 16PC FTIR. The ultraviolet spectra were recorded on a Hewlett–Packard 8450A diode array spectrophotometer. Photolysis was conducted in a Rayonet Photochemical Mini-Reactor chamber Model RMR-600 purchased from the Southern New England Ultraviolet Company (Branford, CT) in 0.7 mL water jacketed quartz cells. Liquid scintillation counting was conducted on a Packard 1900 TR Liquid Scintillation Counter (Meridian, CT).

Caution

Sodium azide and aryl azides are explosive, and hydrazoic acid is explosive and poisonous. Reactions using or generating these reagents should be performed in a well-ventilated hood behind an explosion-proof shield. We have worked with these reagents and procedures on mg to gram scales, and to date have observed no explosions. Nevertheless, use extreme care when repeating or scaling up these procedures. All manipulations of phenylazides were conducted in the dark or under a red light.

2-(4-Azidophenyl)acetaldehyde (5). A solution of 4-azidophenethyl alcohol (**4**, 0.5 g, 3.1 mmol) in dry methylene chloride (2 mL) was added to PDC (2 g, 1.5

equivalent) suspended in dry methylene chloride (2 mL). After stirring at room temperature for 5 hr under nitrogen, the reaction mixture was diluted with ethyl ether (50 mL) The black solid was removed by suction filtration and washed with ethyl ether (50 mL). The combined ether layer was extracted with sodium bicarbonate (10%, 50 mL). The organic layer was evaporated to remove solvent. The product was then purified by silica gel chromatography, eluting with hexane/ethyl acetate (9:1). The appropriate fractions were pooled and roto-evaporated, yielding 0.4 g (80%) of crude product as a yellowish oil. ^{1}H-NMR ($CDCl_3$) δ 3.67 (d, J = 2.1, 2H, C2H), 7.07 (d, J = 6.6, 2H, PhH), 7.18 (d, J = 6.6, 2H, PhH), 9.72 (t, J = 2.1, 1H, C1H).

2-Chloro-2-(4-azidophenyl)acetaldehyde (6): Freshly prepared 4-azidophenylacetaldehyde (**4**, 0.2 g, 1.24 mmol) was dissolved in acetic acid (2 mL), and *t*-butyl hypochlorite (170 μL, 1.1 equivalent) in acetic acid (1 mL) was added dropwise. After stirring 1 hr at room temperature, the reaction mixture was diluted with water (5 mL) and extracted with three volumes of ethyl ether. The combined ether extracts were washed with water until the aqueous phase was neutral, dried, and filtered (do not extract with base as the product decomposes). The final crude product contained 70% aldeyhyde product and 30% acid by NMR: ^{1}H-NMR ($CDCl_3$) δ 5.19 (d, J = 2.7 Hz, 1H, C2H), 6.95–7.21 (m, 4H, PhH), 9.49 (d, J = 2.7 Hz, 1H, C1H).

2-Bromo-2-(4-azidophenyl)acetaldehyde (7). Freshly-prepared 2-(4-azidophenyl)-acetaldehyde (**4**, 0.1g, 0.62 mmol) and *p*-toluenesulfonic acid (about 0.1 equivalent) were dissolved in dry THF (2 mL), and NBS (0.11 g, 1 equivalent) was added in small portions. The reaction was stirred at room temperature until the brown color disappeared (about 30 min). The reaction mixture was diluted with methylene chloride (20 mL) and extracted with three volumes of water. Evaporation of the organic layer yielded the crude product as a yellowish oil. ^{1}H-NMR ($CDCl_3$) δ 5.19 (d, J = 2.7 Hz, 1H, C2H), 6.95–7.21 (m, 4H, PhH), 9.49 (d, J = 2.7 Hz, 1H, C1H).

α-(4-Azidophenyl)-1,N^6-etheno-2′-deoxyadenosine 5′-monophosphate (3m). A solution of dAMP (50 mg, 0.14 mmol) and sodium acetate (0.24 g, 1.76 mmol) in water (1 mL) was added to a 10-fold molar excess of freshly prepared α-halo-2-(4-azidophenyl)acetaldehyde (**6** or **7**) in acetonitrile (1 mL), and the heterogeneous solution was stirred at 40°C for 24 hr. The reaction was then diluted with water (10 mL), neutralized with 0.1N NaOH and extracted with three volumes of ethyl ether. The aqueous phase was lyophilized, and the product was purified by ion-exchange chromatography on a DEAE-sephadex column with an average purification yield of 20%: IR (KBr) 2120 (N_3); UV λ_{Max} ($\varepsilon \times 10^{-4}$): 0.05N NaOH, 275 (1.46), 298 (1.96); 0.05N HCl, 275 (1.72), 298 (1.93); 0.01M ammonium acetate, 276 (1.38), 296 (1.83); 1H-NMR δ 2.58 (m, 1H, C2′H1), 2.88 (m, 1H, C2′H2), 3.97 (t, J = 3.9 Hz, 2H, C5′H), 4.21 (m, 1H, C4′H), 4.68 (br s, 1H, C3′H), 6.55 (t, J = 6.9 Hz, 1H, C1′H), 7.01 (d, J = 7.8 Hz, 2H, PhH), 7.46 (d, J = 7.8 Hz, 2H, PhH), 7.50 (s, 1H, C10H), 8.52 (s, 1H, C2H), 8.92 (s, 1H, C8H); high resolution FAB-MS m/e 471.0953; calcd. for $C_{18}H_{16}N_8O_6P_1$ ($M-H^+$), 471.0930.

α-(4-Azidophenyl)-1,N^6-etheno-2′-deoxyadenosine 5′-triphosphate (3) was synthesized from dATP and a 10-fold molar excess of **6** (or **7**) as described in the synthesis of **3** with an average yield of 20%, or by the pyrophosphorylation of **4m** as described

in the synthesis of **2**[2] with yield of about 50%. The product was purified by either preparative HPLC eluting from a C4 column with 0–50% acetonitrile in 10 mM triethylammonium bicarbonate, pH 7.5, or by FPLC ion-exchange chromatography eluting from Mono-Q column with a 0.1–1.6 M ammonium acetate, pH 8.0 gradient. The final product was >95% pure based on elution from analytical reverse phase HPLC in the solvent given above: MS (-FAB, glycerol) m/e 631 ($M-H^+$).

Photochemistry

Nucleotide monophosphate (**3m**, $\sim$ 0.5 mM) was dissolved in distilled water (800 μL) and irradiated at 3000 Å at room temperature in a quartz cuvette or in a clear polypropylene tube. At indicated time points, aliquots of 50 μL were removed and diluted in 0.1 N HCl (2.95 mL). The UV spectra of the diluted samples were measured; the absorbance at 293 nm was plotted as a function of time and the half-life for photodecomposition was calculated by fitting the data to a first order kinetic equation.

Structure and Conformation of TCPI 3

Nucleotide α-phenyl-1,N^6-etheno-dAMP was synthesized from dAMP and α-bromo-phenylacetaldeyde by the method used to synthesize the 4-azido analog **3m**. The regiochemistry of the phenyl ring was deduced using the NOE difference spectra observed after selective irradiation of the C2 proton.

The solution structure of the polymerase inhibitor **3m** was studied by molecular mechanics calculations as described earlier for nucleotides **1**[5] and **2**.[7] Briefly, Sybyl 6.0 (Tripos Associates, Inc., St. Louis, MO) computations were run on IBM's UNIX variant AIX (version 4.25). TCPI **3** was constructed by modification of the structure of dAMP taken from BIOPOLYMER. Semi-empirical calculations were performed using the MOPAC package and MNDO method to optimize the charge and geometry of nucleotide. Potential energy calculations of purine analogues were performed using the Tripos force field, and those of nucleotide analogues were performed using the Kollman all atom force field[19,20] with addition of the $C_{4'}$-$O_{4'}$-$C_{1'}$-N* anomeric torsional parameters for cyclic compounds to correct for the anomeric effect.[21] A dielectric constant of 1 was used in these calculations. Systematic sampling of torsional space was accomplished using the GRID SEARCH option in Sybyl 6.0. The criterion for termination of minimization was an energy change less than 0.0001 kcal/mol. The conformations generated by grid search were analyzed using the MOLECULAR SPREADSHEET function, which allows the measurement and calculation of parameters such as torsional angels, interproton distances, and the pseudorotational phase angle P.[15]

Polymerase Assays

For assay of the polymerase activity of the Klenow fragment, poly(dA) · $(dT)_{10}$ and thymidine 5′ triphosphate (TTP) were used as template/primer and nucleoside triphosphate substrate, respectively, as previously described.[1] Briefly, reaction mixtures containing 10 concentrations of template/primer (from 5–50 nM in 0.5 Km increments), a fixed concentration of ^{3}H-TTP (25 μM), and in the absence and presence of various concentrations of inhibitor **3** (0–19 μM) or dATP (0–200 μM)

were intiated by addition of 2.6 E-4 units of KF in a total volume of 25 μL and incubated in 50 mM tris-HCl buffer, pH 7.4, containing 3 mM magnesium chloride and 1 mg/mL BSA at 37°C for 30 min. The reactions were terminated by addition of 25 μL of 30 mM EDTA solution, pH 8, and quenched aliquots (10 μL) were spotted on DEAE cellulose filter paper (squares of 2×2 cm^2 or 2.5 cm diameter circles). The filter papers were washed three times in ammonium formate solution (0.3 M, pH 8, >5 mL/square) with gentle stirring, dehydrated in ethanol and ethyl ether and air-dried. The radioactivity on each filter paper was then measured in triplicate by scintillation counting in 5 mL of Scintiverse II. The initial rate was determined as the picomoles of [^{3}H]TTP incorporated into DNA per min. The initial velocity versus substrate concentration data were fit to a MM equation using non-linear regression analysis in KINETICS to determine Km and Vmax. Inhibition data (40 datapoints per assay) was fit by non-linear regression analysis to competitive, non-competitive, uncompetitive, and mixed inhibition models, and the best fit was chosen based on statistical parameters (r^2, cod, and model selection criterion). The Ki's reported are the average of three determinations.

The polymerase activity of HIV-1 reverse transcriptase was assayed using poly(rA) · $(dT)_{10}$ as template/primer and TTP as the nucleoside triphosphate substrate as previously described.[2] For IC_{50} assays, RT (2.4 E-4 units) in 50 mM tris-HCl buffer (pH 7.4) containing 3 $MgCl_2$ and 1 mg/mL of BSA was incubated with template/primer (20 nM) and ^{3}H-TTP (25 μM) for 30 min, and radioactivity incorporated into DNA was determined by the DEAE absorption method as described above for the DNA pol assay. IC_{50}'s were determined at 10 concentrations of inhibitor over 2.5 log units from 0 to 100% inactivation or up to solubility limits (for monophosphates) or up to 300 μM (for triphosphates). Non-linear regression analysis using the method of Chou[22] was used to determine the IC_{50}'s, and the average and standard error of at least triplicate determinations is reported.

For irreversible photo-inactivation studies, a standard irradiation mixture contained 2 μM KF, β-mercaptoethanol (BME), 3 mM magnesium chloride and the photoprobe (100 μM) in 100 mM Tris-HCl buffer (pH7.4) in a total volume of 40 μL; for substrate protection experiments, saturating (2000 nM) template-primer was added to the photolysis mixture. The concentration of BME used in the photolysis was 20 times the photoprobe or 2 mM in the absence of the inhibitor. The photolysis mixture was incubated at 37°C for 10 min in the dark and irradiated at 3000 Å at 25°C. Aliquots of 5 μL were removed at indicated times and diluted 10-fold in the assay buffer. An aliquot (5 μL) of the diluted sample was assayed for polymerase activity in a total volume of 50 μL using 20 nM of template/primer and 25 μM [^{3}H]-TTP. The % photoinactivation at each time point was calculated as the percentage loss of enzyme activity relative to the enzyme activity of the control in which the enzyme was photolyzed in the absence of the photoprobe.

REFERENCES

1. Moore, B.M.; Li, K.; Doughty, M.B. Deoxyadenosine-based DNA polymerase photoprobes: design, synthesis and characterization as inhibitors of DNA polymerase I Klenow fragment. Biochemistry **1996**, *35*, 11634–11641.
2. Li, K.; Lin, W.; Chong, K.H.; Moore, B.M.; Doughty, M.B. Template-competitive

inhibitors of HIV-1 reverse transcriptase: design, synthesis and inhibitory activity. Bioorganic Med. Chem. **2002**, *10*, 507–515.
3. Doronin, S.V.; Lavrik, O.I.; Nevinsky, G.A.; Podust, V.N. The efficiency of dNTP complex formation with human placenta DNA polymerase α as demonstrated by affinity modification. FEBS Lett. **1987**, *216*, 221–224.
4. Kolocheva, T.I.; Nevinsky, G.A.; Levina, A.S.; Khomov, V.V.; Lavrik, O.I. The mechanism of recognition of templates by DNA polymerases from pro-and eukaryotes as revealed by affinity modification data. J. Biomol. Struc. Dyn. **1991**, *9*, 169–186.
5. Moore, B.M.; Jalluri, R.; Doughty, M.B. DNA Polymerase photoprobe 2-(4-azidophenacyl)thio-dATP identifies the template binding region of the DNA polymerase I Klenow fragment. Biochemistry **1996**, *35*, 11642–11651.
6. Lin, W.; Li, K.; Doughty, M. Characterization of a binding site for template competitive inhibitors of HIV-1 reverse transcriptase using photolabeling derivatives. Bioorganic Med. Chem. **2002**, *10*, 4131–4141.
7. Lin, W.; Li, K.; Moore, B.M.; Doughty, M.B. Conformational properties of template competitive HIV-1 reverse transcriptase inhibitors: analysis of enzyme binding modes. Nucleosides Nucleotides Nucleic Acids **2003**, *22*, 283–297.
8. Lewis, R.V.; Roberts, M.F.; Dennis, E.A.; Allison, W.S. Photoactivated heterobifunctional cross-linking reagents which demonstrate the aggregation state of phospholipase A. Biochemistry **1979**, *16*, 5650–5654.
9. Mancuso, A.J.; Swern, D. Activated dimethyl sulfoxide: useful reagents for synthesis. Synthesis **1981**, 165–185.
10. Corey, E.J.; Schmidt, G. Useful procedures for the oxidation of alcohols involving pyridinium dichromate in aprotic media. Tetrahedron Lett. **1979**, *20*, 399–402.
11. Hanze, A.R.; Fonken, G.S.; McIntosh, J.A.V.; Searcy, A.M.; Levin, R.H. Chemical studies with 11-oxygenated steroids. V. A one-step oxidation-halogenation of 3-hydroxysteroids. J. Am. Chem. Soc. **1954**, *76*, 3179–3181.
12. Schram, K.H.; Townsend, L.B. Fluorescent nucleoside derivatives of imidazo[1,2-C]pyrrolo[2,3-d]pyrimidine: a new and novel heterocyclic ring system (1). Tetrahedron Lett. **1974**, *15*, 1345–1348.
13. Meyer, R.B., Jr.; Shuman, D.A.; Robins, R.K.; Miller, J.P.; Simon, L.N. Synthesis and enzymic studies of 5-aminoimidazole and N-1-and N-6-substituted adenine ribonucleoside cyclic 3′,5′-phosphates prepared from adenosine cyclic 3′,5′-phosphate. J. Med. Chem. **1973**, *16*, 1319–1323.
14. Jones, G.H.; Murthy, D.V.K.; Tegg, D.; Golling, R.; MOffatt, J.G. Analogs of adenosine 3′,5′-cyclic phosphate, II. Synthesis and enzymatic activity of derivatives of 1,N^6-ethenoadenosine 3',5'-cyclic phosphate. Biochem. Biophys. Res. Commun. **1973**, *53*, 1338–1343.
15. de Leeuw, H.P.M.; Haasnoot, C.A.G.; Altona, C. Empirical correlations between conformational parameters in β-D-furanoside fragments derived from a statistical survey of crystal structures of nucleic acid constituents. Full description of nucleoside molecular geometries in terms of four parameters. Isr. J. Chem. **1980**, *20*, 108–126.
16. Pelletier, H.; Sawaya, M.R.; Kumar, A.; Wilson, S.H.; Kraut, W.J. Structures of ternary complexes of rat DNA polymerase β, a DNA template-primer, and ddCTP. Science **1994**, *264*, 1891–1903.

17. Huang, H.; Chopra, R.; Verdine, G.L.; Harrison, S.C. Structure of a covalently trapped catalytic complex of HIV-1 reverse transcriptase: implications for drug resistance. Science **1998**, *282*, 1669–1675.
18. Teeter, H.M.; Bell, E.W. tert-Butyl hypochlorite. Org. Synt. **1952**, *32*, 20–22.
19. Weiner, S.J.; Kollman, P.A.; Case, D.A.; Singh, U.C.; Ghio, C.; Alagona, G.; Profeta, S.; Weiner, P. A new force field for molecular mechanical simulation of nucleic acids and proteins. J. Am. Chem. Soc. **1984**, *106*, 765–784.
20. Weiner, S.J.; Kollman, P.A.; Nguyen, D.T.; Case, D.A. An all atom force field for simulations of proteins and nucleic acids. J. Comput. Chem. **1985**, *7*, 230–252.
21. Jalluri, R.K.; Yuh, Y.H.; Taylor, E.W. O-C-N anomeric effect in nucleosides: a major factor underlying the experimentally observed eastern barrier to pseudorotation. In *The Anomeric Effect and Associated Steroelectronic Effects*; Thatcher, G.R.J., Ed.; American Chemical Society: Washington, 1993; 277–293.
22. Chou, T.-C. Relationships between inhibition constants and fractional inhibition in enzyme-catalyzed reactions with different numbers of reactants, different reaction mechanisms, and different types and mechanism of inhibition. Mol. Pharmacol. **1974**, *10*, 235–247.